Supplementary Information for Transitional calcite-aragonite stacking as a signature of hexagonal aragonite in biogenic and inorganic deposits

Author Information

Péter Németh[1, 2] *, Attila Demény[1], Péter Pekker[2,3], Aleksander Rečnik[4], Vesna Ribić[4], Pavel N. Gavryushkin[5,6], Maksim Banaev[5,6], Marco Bruno[7], Christoph Spötl[8], Michael Pettauer[9], Martin Dietzel[9], Levente Illés[10], Mihály Pósfai[2,3]

Affiliations

[1] Institute for Geological and Geochemical Research, HUN-REN REN Research Centre for Astronomy and Earth Sciences (MTA Centre of Excellence), Budapest, Hungary

[2] Research Institute of Biomolecular and Chemical Engineering, University of Pannonia, Veszprém, Hungary

[3] HUN-REN–PE Environmental Mineralogy Research Group, Veszprém, Hungary

[4] Department for Nanostructured Materials, Jožef Stefan Institute, Ljubljana, Slovenia

[5] V.S. Sobolev Institute of Geology and Mineralogy, Siberian Branch of Russian Academy of Sciences, Novosibirsk, Russia

[6] Novosibirsk State University, Novosibirsk, Russia

[7] Department of Earth Sciences, University of Turin, Turin, Italy

[8] Institute of Geology, University of Innsbruck, Innsbruck, Austria

[9] Institute of Applied Geosciences, Graz University of Technology, Graz, Austria

[10] Institute of Technical Physics and Materials Science, HUN-REN Centre for Energy Research, Budapest, Hungary.

Correspondence to: *Péter Németh, nemeth.peter@csfk.org

This PDF file includes:

Fig. 8. Starting models of a (001) aragonite SF, built by insertion of various aragonite (V04.1, V05.1, V05.2) and calcite (V06) slabs.
Fig. S9: DFT-calculated structure models of two (001) aragonite SFs, built by insertion of various aragonite (V04.1, V05.1, V05.2) and calcite (V06) slabs.

Supplementary Table 1. Stable carbon and oxygen isotope compositions (in ‰ relative to V-PDB) of the L-top sample collected at the Berger Károly Cave[14], the Sonnenberg (LAS34b[47]) and the Erzberg[15] samples.

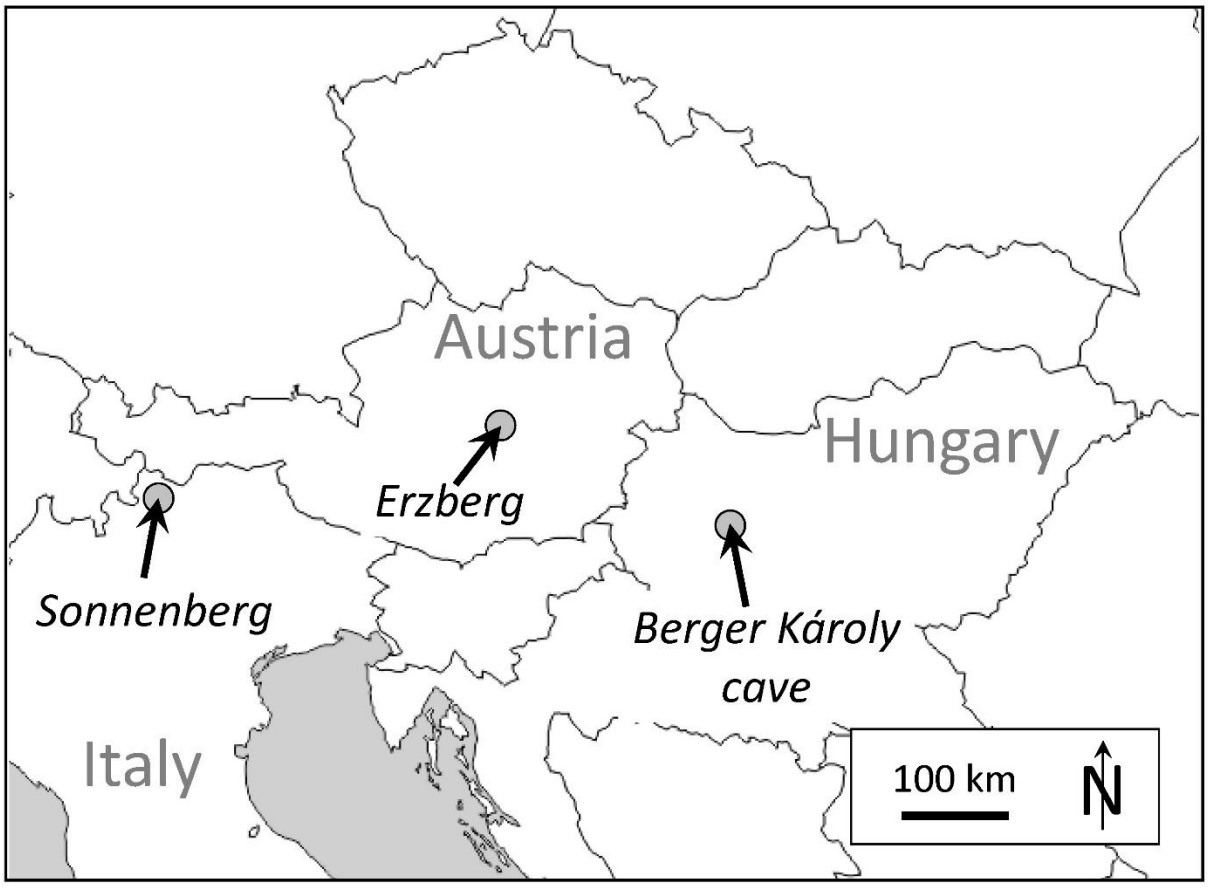

Fig. S1a. Localities of the sample collection sites.

Fig. S1b. Lángos Lake in the Berger Károly Cave. The L-top sample was drilled into the calcite deposit covering this pool (marked by a white arrow). The drill core contains mainly dense calcite, covered by microbial calcite encrustation, an aragonite layer, and a final calcite layer (see also Fig. S2).

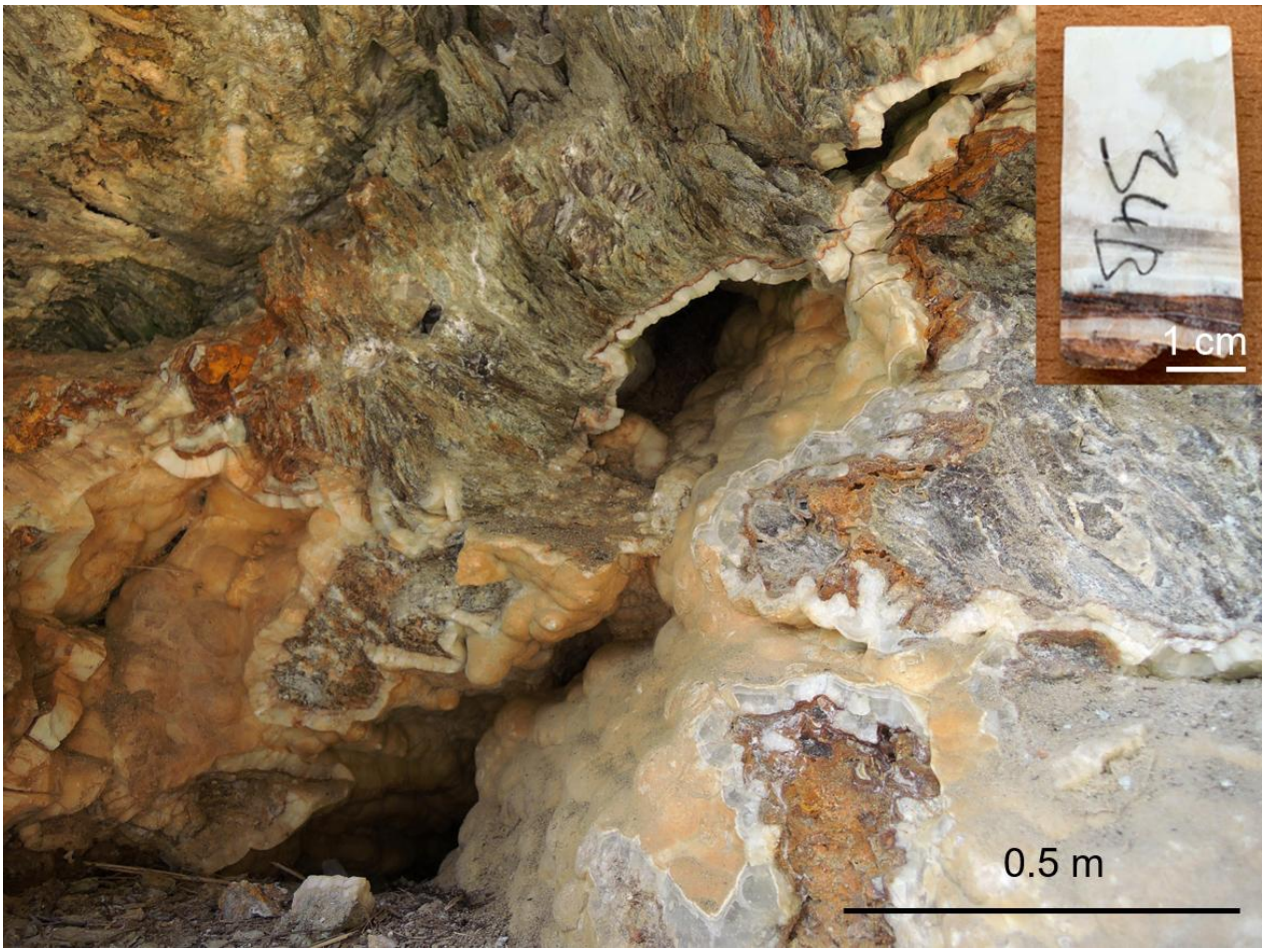

Fig. S1c. Calcite-aragonite flowstone in an extensional fracture at the Sonnenberg site (Italy) where sample LAS34 was obtained. Inset: detail of sample LAS34.

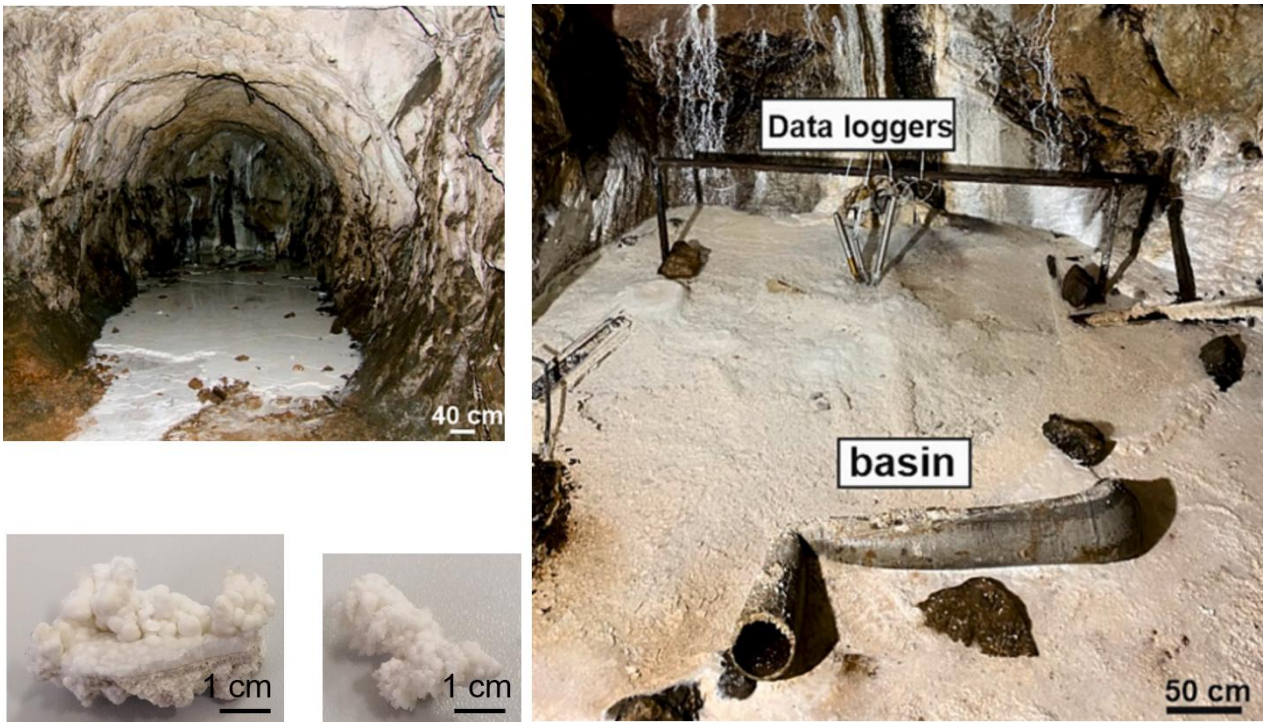

Fig. S1d. Modern calcite-aragonite precipitates in an artificial pool in an abandoned tunnel of the Erzberg mine (Austria).

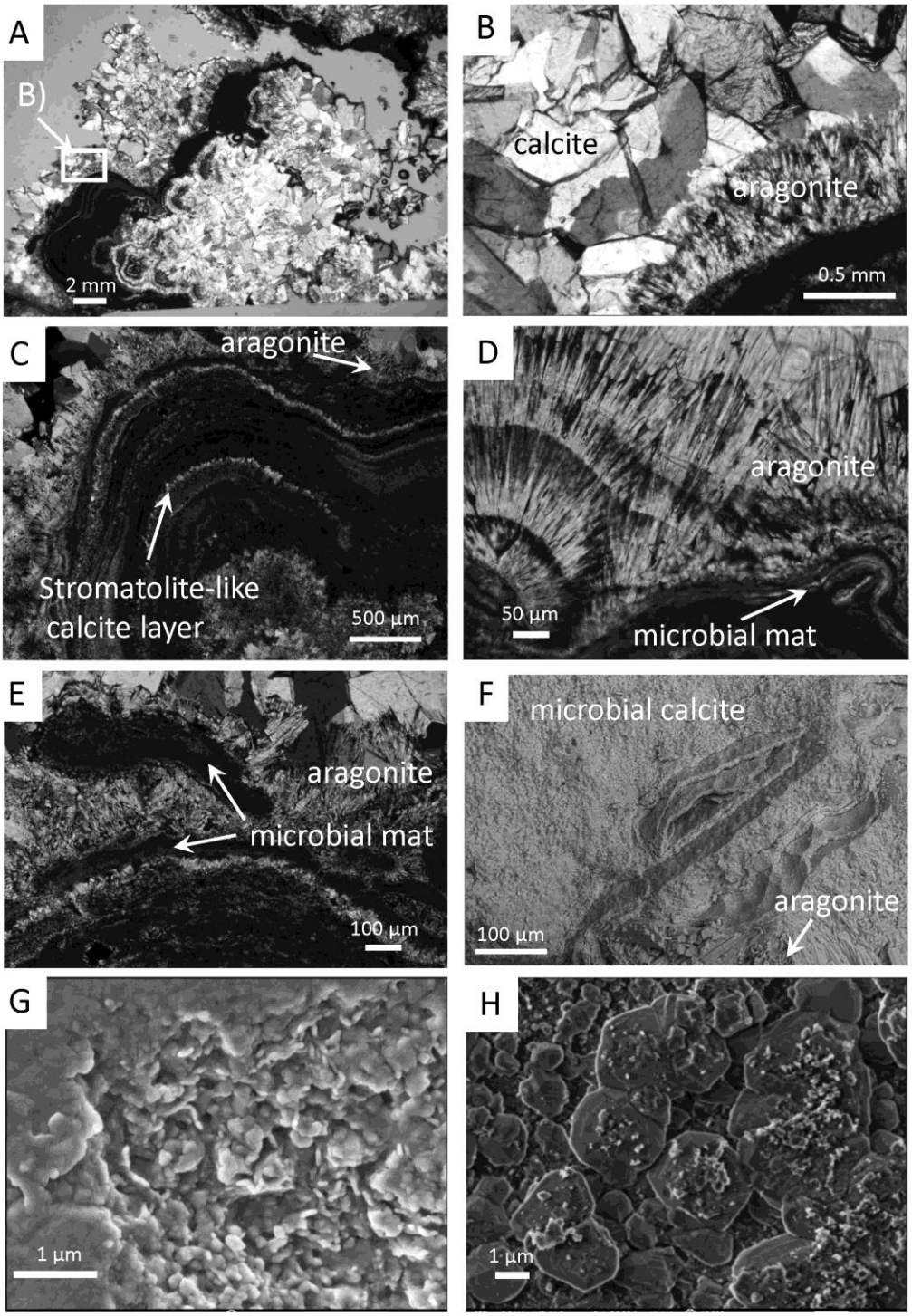

Fig. S2a: Transmitted-light microscopy images (partially crossed nicols in A, crossed nicols in B-E) of the topmost layer of sample L-top, Berger Károly cave and scanning electron microscopic images of the boundary between aragonite and microbial calcite (F), the bottom of the aragonite layer (G) and the top of the microbial calcite layer (H).

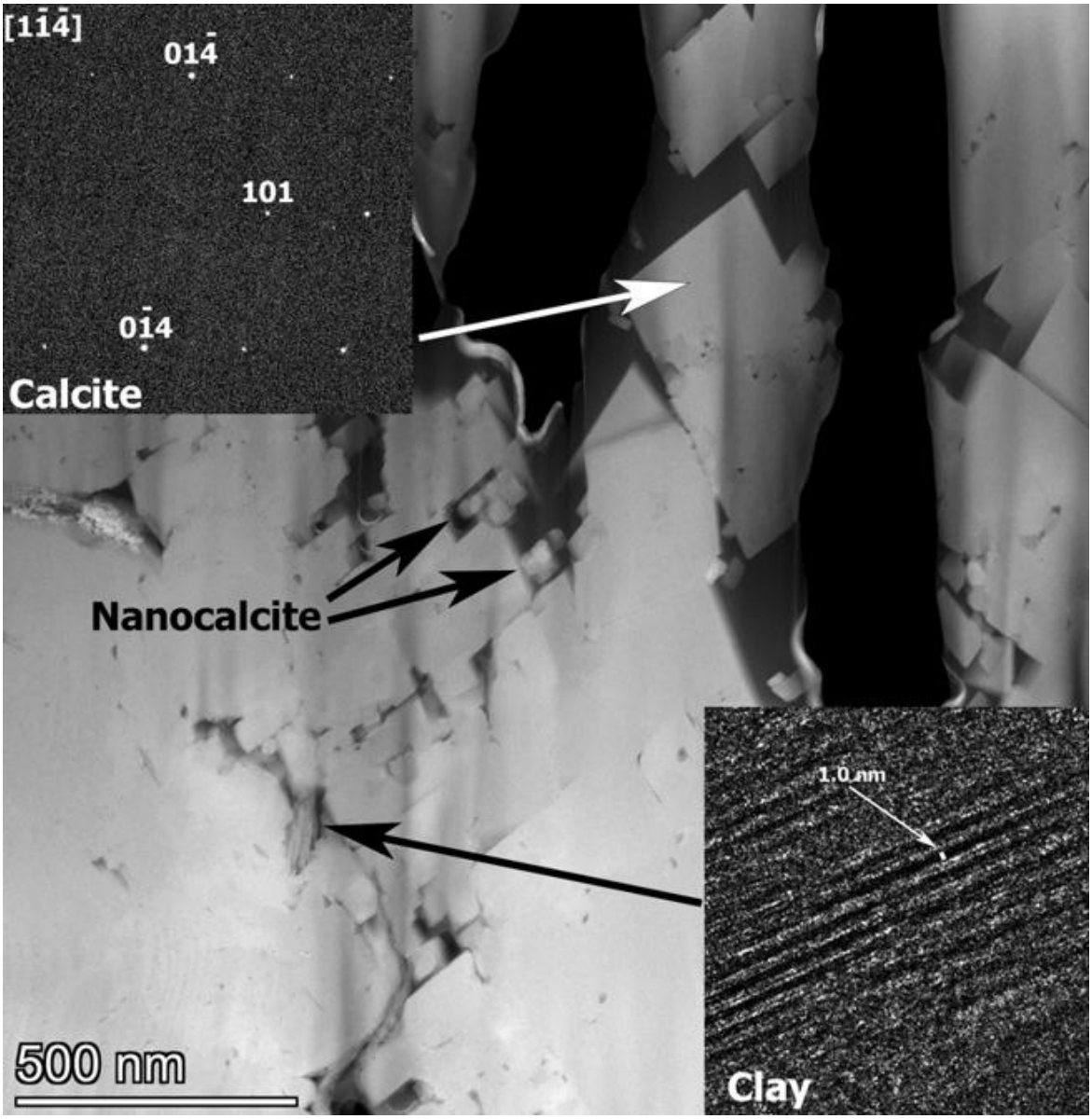

Fig. S2b: STEM image and SAED pattern from the last-grown calcite (Berger-Károly cave). The HRTEM image of the bottom right insert shows a clay mineral with 1 nm spacings.

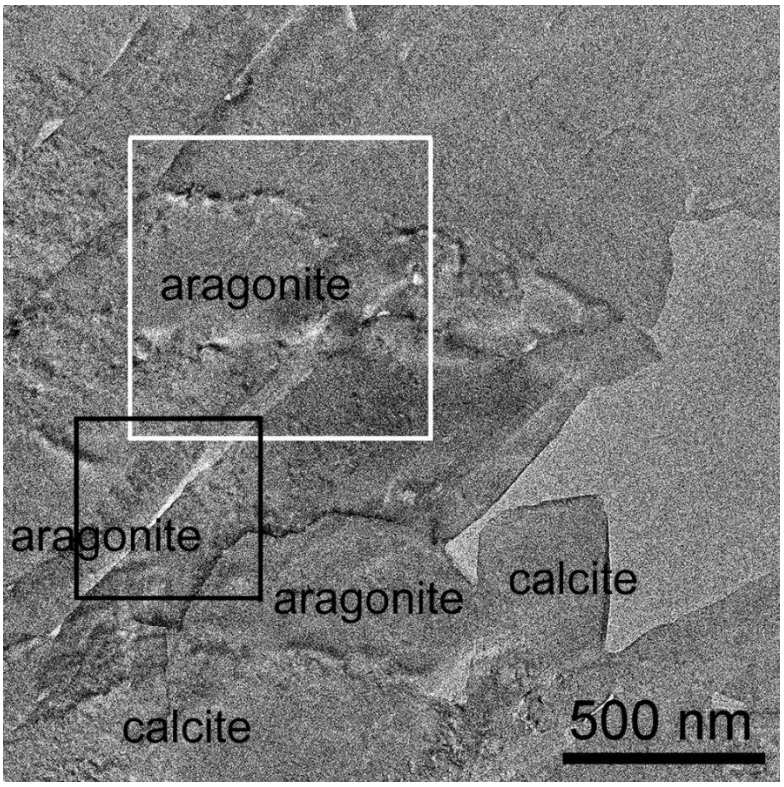

Fig. S3: BFTEM image of the FIB lamella obtained from the calcite-aragonite boundary (Berger-Károly cave). Black and white rectangles mark the areas magnified in Fig. 2 and Fig. S4, respectively.

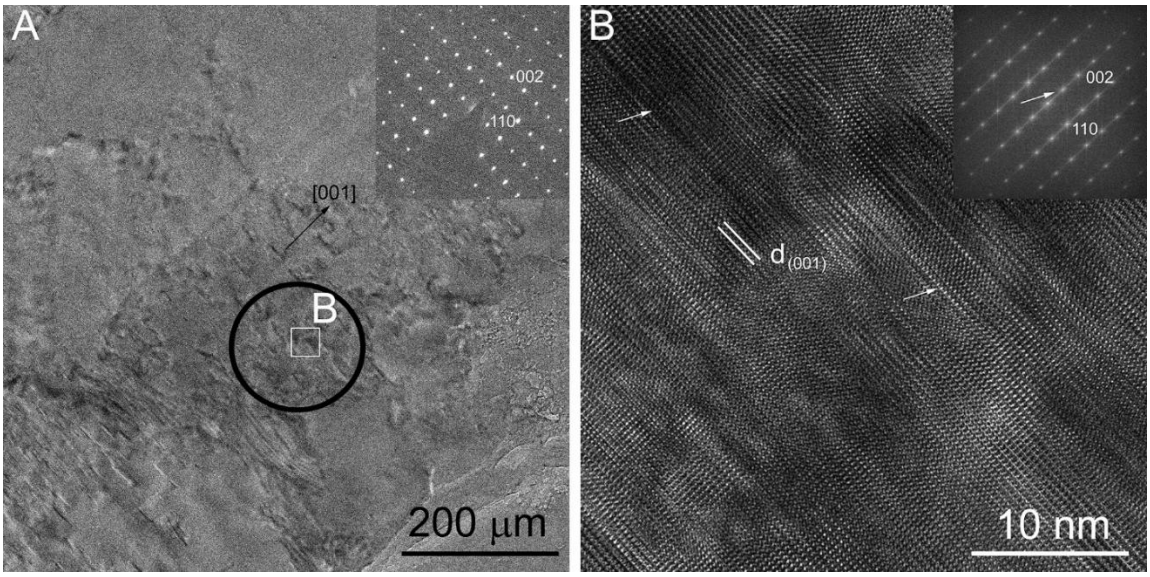

Fig. S4: (001) aragonite SFs viewed along aragonite [1-10] (Berger Károly cave). A: BFTEM image obtained from the area marked by white rectangle in Fig. S3. The SAED pattern taken from the black open circle shows aragonite viewed along [1-10]. B: HRTEM image obtained from the area marked by the white rectangle in A.

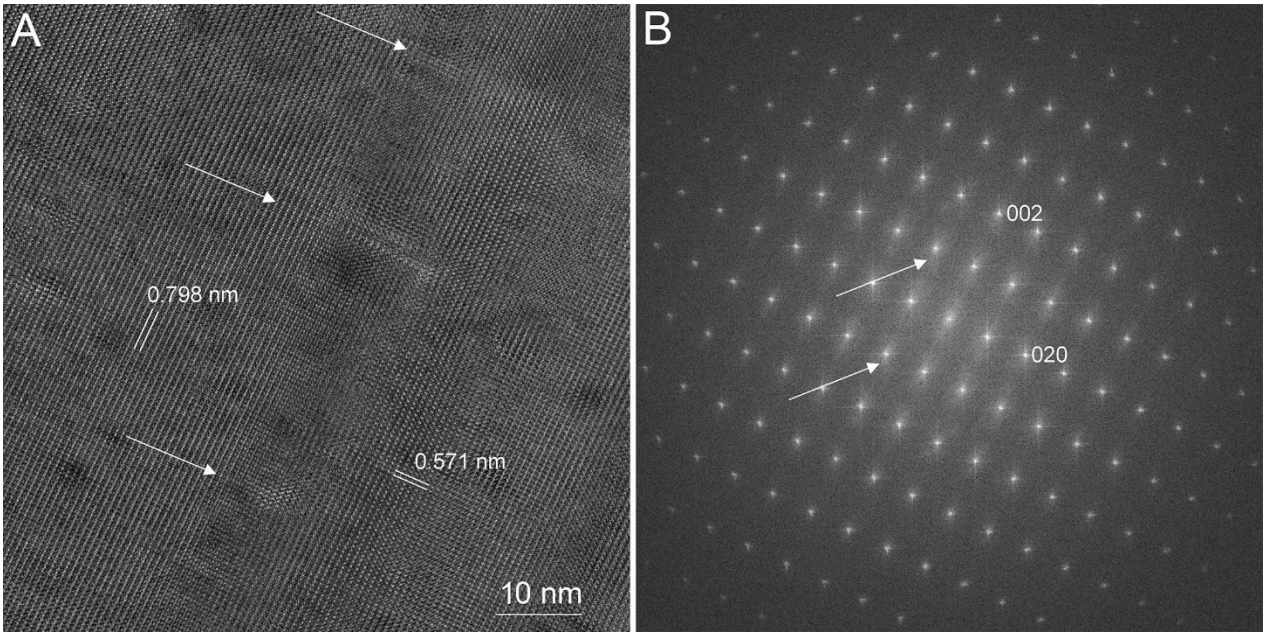

Fig. S5: (001) aragonite SFs from Sonnenberg. A: HRTEM image obtained from the area marked by the white rectangle in Fig. 5A. B: FFT calculated from A. White arrows point to SFs (A) and streaked reflections (B).

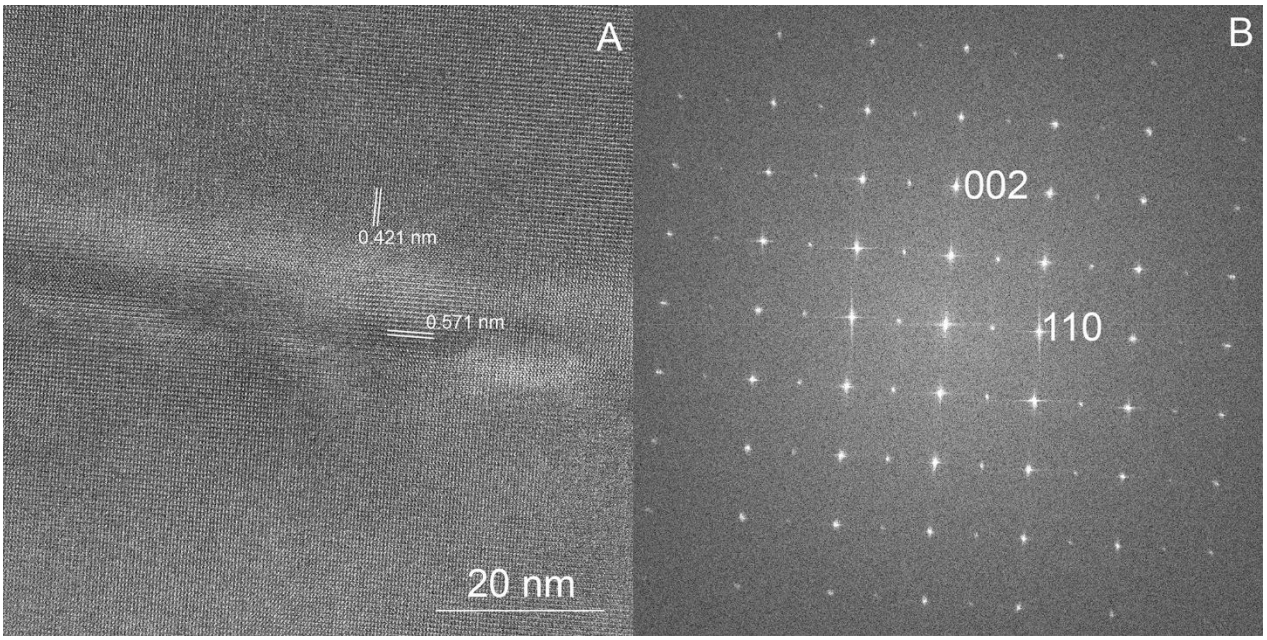

Fig. S6: Defect-free aragonite from Erzberg. A: HRTEM image obtained from the area marked by white rectangle in Fig. 5B. FFT calculated from A. Streaked reflections are invisible (B) and the undulating contrast of A presumably indicates a grain boundary.

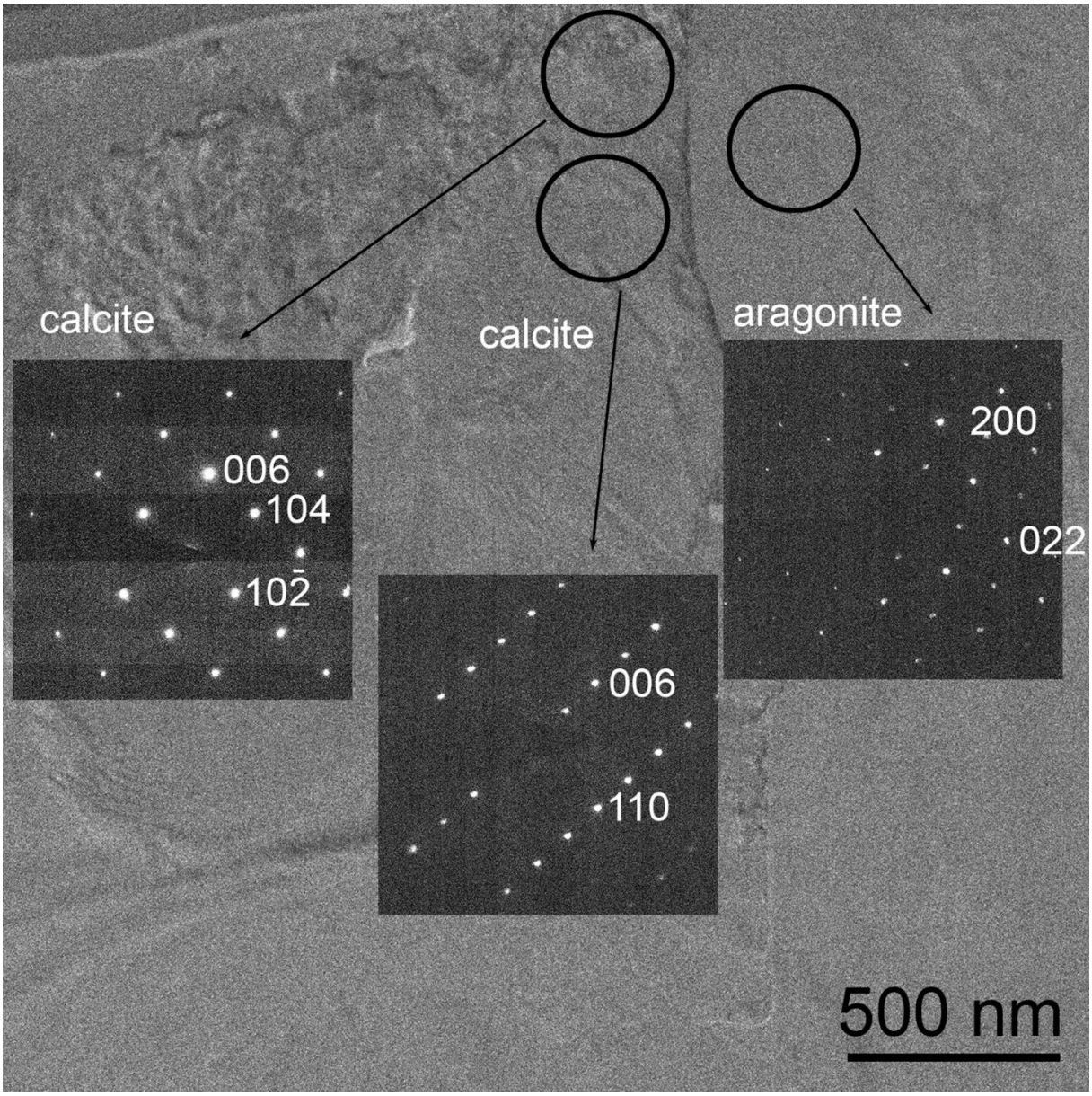

Fig. S7: BFTEM image and SAED patterns of the first grown aragonite and last grown calcite (Sonnenberg) from TEM2 lamella shown in Fig. 1E.

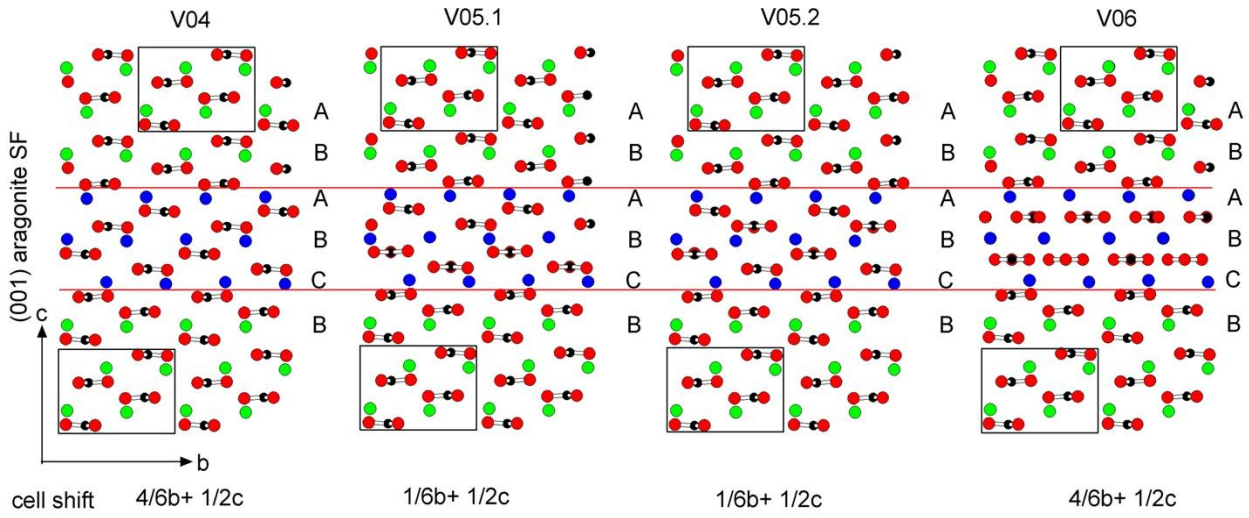

Fig. S8. Starting models of a (001) aragonite SF, built by insertion of various aragonite (V04.1, V05.1, V05.2) and calcite (V06) slabs.

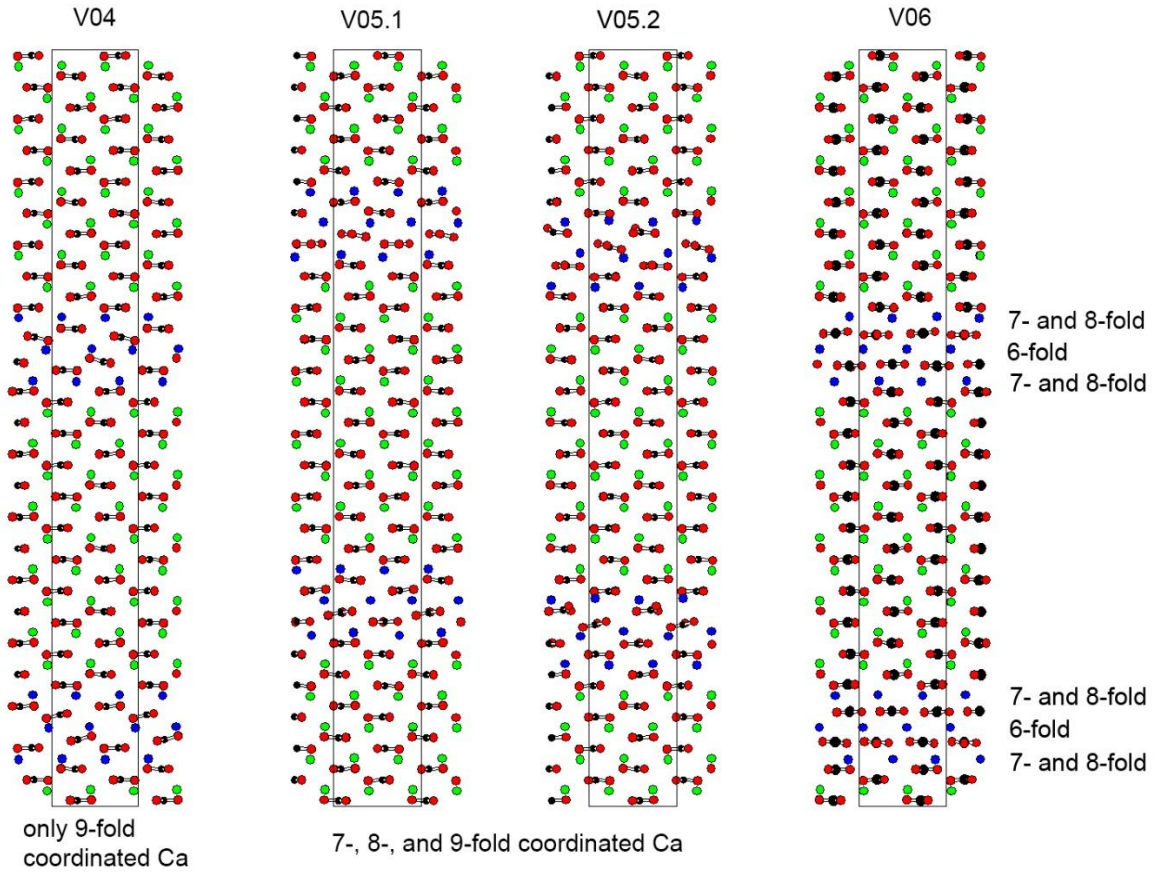

Fig. S9: DFT-calculated structure models of two (001) aragonite SFs, built by insertion of various aragonite (V04, V05.1, V05.2) and calcite (V06) slabs.

Supplementary Table 1. Stable carbon and oxygen isotope compositions (in ‰ relative to V-PDB) of the L-top sample collected at the Berger Károly Cave[14], the Sonnenberg (LAS34b[47]) and the Erzberg[15] samples.

		$\delta^{13}C$	$\delta^{18}O$
L-top-3	drusy calcite	-4.3	-10.8
L-top-1	drusy calcite	-3.0	-10.9
L-top-2	drusy calcite	-4.1	-10.6
L-top-4	aragonite	-6.0	-9.2
L-top-5	aragonite	-5.4	-9.8
L-top-6	aragonite-calcite boundary	-2.8	-10.7
L-top-7	yellow microbial calcite	-2.6	-10.9
L-top-8	yellow microbial calcite	-2.8	-10.8
L-top-9	yellow microbial calcite	-2.7	-10.9
L-top-10	yellow microbial calcite	-3.1	-10.6
L-top-11	boundary	-3.5	-8.8
L-top-12	laminated calcite	-2.5	-7.0
L-top-13	laminated calcite	-2.3	-6.7
L-top-14	laminated calcite	-2.6	-7.1
L-top-15	boundary	-2.9	-7.8
L-top-16	dense calcite	-3.2	-8.6
L-top-17	dense calcite	-3.4	-9.0
L-top-18	dense calcite	-3.4	-9.6
LAS34b1	aragonite	4.4	-10.4
LAS34b2	aragonite-calcite boundary	2.2	-11.2
LAS34b3	calcite	1.0	-12.2
LAS34b4	calcite	1.5	-11.9
LAS34b5	calcite	1.9	-11.7
LAS34b6	aragonite	5.2	-10.7
Erzberg	aragonite	0.6	-8.0